Inorg. Chem. **2006**, *45*, 6523–6534

Mechanistic Studies on the Nitrite-Catalyzed Reductive Nitrosylation of Highly Charged Anionic and Cationic Fe^{III} Porphyrin Complexes

Joo-Eun Jee and Rudi van Eldik*

Institute for Inorganic Chemistry, University of Erlangen-Nürnberg, Egerlandstrasse 1, 91058 Erlangen, Germany

Received February 23, 2006

The nitrosyl complexes formed during the binding of NO to the $(P^{n})Fe^{III}(H_2O)_2$ (n = 8+ and 8–) complexes, viz., $(P^{8-})Fe^{II}(H_2O)(NO^{+})$ and $(P^{8+})Fe^{II}(H_2O)(NO^{+})$, undergo subsequent reductive nitrosylation reactions that were found to be catalyzed by nitrite, which was also produced during the reaction. The effect of the nitrite concentration, pH, temperature, and pressure on the nitrite-catalyzed reductive nitrosylation process was studied in detail for $(P^{8-})Fe^{III}(H_2O)_2$, $(P^{8+})Fe^{III}(H_2O)_2$, and $(P^{8+})Fe^{III}(OH)(H_2O)$, from which rate and activation parameters were obtained. On the basis of these data, we propose mechanistic pathways for the studied reactions. The available results favor the operation of an innersphere electron-transfer process between nitrite and coordinated NO^{+}. By way of comparison, the cationic porphyrin complex $(P^{8+})Fe^{III}(L)_2$ (L = H_2O or OH^{-}) was found to react with NO_2^{-} to yield the nitrite adduct $(P^{8+})Fe^{III}(L)(NO_2^{-})$. A detailed kinetic studied revealed that nitrite binds to $(P^{8+})Fe^{III}(H_2O)_2$ according to a dissociative mechanism, whereas nitrite binding to $(P^{8+})Fe^{III}(OH)(H_2O)$ at higher pH follows an associative mechanism, similar to that reported for the binding of NO to these complexes.

Introduction

In general, nitrite can interfere with the binding of NO to transition-metal complexes, for example, as reported for aquacobalamin (vitamin B_{12a}), where it was found that the observed reactions were solely due to the interaction with nitrite impurities in aqueous NO solutions.[1] Nitric oxide is a versatile signaling molecule that binds reversibly to cytochrome c oxidase (complex IV); its action ranges from hemodynamic regulation to antiproliferative roles on vascular smooth muscle cells. NO transfer in human hemoglobin from the heme to cysteine thiols in cys β-93 to form bioactive nitrosothiols leads to the formation of SNO−Hb, in which reductive nitrosylation provides a pathway for S-nitrosation.[2−7] It has been proposed to be reversible and includes considerable implications, especially in playing a major factor in vasodilation and platelet inhibition. Redox activation of the NO molecule is needed in order for this transfer to occur.[2−7] In recent investigations on the reactions of NO, it was reported that the electronic nature, steric effect, structure and overall charge of the porphyrin ligand bound to the iron(III) center play a major role in determining the reactivity of NO.[8−16]

* To whom correspondence should be addressed. E-mail: vaneldik@chemie.uni-erlangen.de.

(1) (a) Wolak, M.; Stochel, G.; Hamza, M.; van Eldik, R. *Inorg. Chem.* **2000**, *39*, 2018. (b) Firth, R. A.; Hill, H. A. O.; Pratt, J. M.; Williams, R. J. P.; Jackson , W. R. *Biochemistry* **1967**, *6*, 2178.

(2) (a) Weichsel, A.; Maes, E. M.; Andersen, J. F.; Valenzuela, J. G.; Shokhireva, T. K.; Walker, F. A.; Montfort, W. R. *Proc. Natl. Acad. Sci. U.S.A.* **2005**, *102*, 594. (b) Gladwin, M. T.; Lancaster, J. R., Jr.; Freeman, B. A.; Schechter, A. N. *Nat. Med.* **2003**, *9*, 496.

(3) Luchsinger, B. P.; Rich, E. N.; Gow, A. J.; Williams, E. M.; Stamler, J. S.; Singel, D. J. *Proc. Natl. Acad. Sci. U.S.A.* **2003**, *100*, 461.

(4) Beltran, B.; Orsi, A.; Clementi, E.; Moncade, S. *Br. J. Pharmacol.* **2000**, *129*, 953.

(5) (a) Stamler, J. S.; Simon, D. I.; Osborne, J. A.; Mullins, M. E.; Jaraki, O.; Michel, T.; Singel, D. J.; Loscalzo, J. *Proc. Natl. Acad. Sci. U.S.A.* **1992**, *89*, 444. (b) Stamler, J. S.; Jaraki, O.; Osborne, J.; Simon, D. I.; Keaney, J.; Vita, J.; Singel, D.; Valeri, R.; Loscalzo. J. *Proc. Natl. Acad. Sci. U.S.A.* **1992**, *89*, 7674.

(6) Stamler, J. S.; Jia, L.; Eu, J. P.; Mcmahon, T. J.; Demchenko, I. T.; Bonaventura, J.; Gernert, K.; Piantadosi, C. A. *Science* **1997**, *276*, 2034.

(7) Tran, D.; Skelton, B. W.; White, A. H.; Lavermann, L. E.; Ford, P. C. *Inorg. Chem.* **1998**, *37*, 2505.

(8) Lim, M. D.; Lorkovic, I. M.; Ford, P. C. *J. Inorg. Biochem.* **2005**, *99*, 151.

(9) Ford, P. C.; Fernandez, B. O.; Lim, M. D. *Chem. Rev.* **2005**, *105*, 2439.

(10) (a) Jee, J.-E.; Wolak, M.; Balbinot, D.; Jux, N.; Zahl, A.; van Eldik, R. *Inorg. Chem.* **2006**, *45*, 1326. (b) Jee, J.-E.; Eigler, S.; Jux, N.; Wolak, M.; Zahl, A.; Stochel, G.; van Eldik, R. *Inorg. Chem.* **2005**, *44*, 7717. (c) Guldi, D. M.; Rahman, G. M. A.; Jux, N.; Balbinot, D.; Hartnagel, U.; Tagmatarchis, N.; Maurizio, P. *J. Am. Chem. Soc.* **2005**, *127*, 9830.

(11) Yoshimura, T.; Suzuki, S.; Nakahara, A.; Iwasaki, H.; Masuko, M.; Matsubara, T. *Biochemistry* **1986**, *25*, 2436.

10.1021/ic0603104 CCC: $33.50
Published on Web 07/04/2006

Scheme 1. General Reaction Sequence Suggested for the Nitrite-Catalyzed Reductive Nitrosylation of $(P)Fe^{II}(NO^+)$

$$(P)Fe^{III} + NO \underset{}{\overset{K_{NO}}{\rightleftharpoons}} (P)Fe^{II}(NO^+) + HONO/NO_2^- \xrightarrow{k_{nit}} (P)Fe^{II}(NO) + NO_x \text{ products}$$

The binding of NO to an Fe(III)[12−14,17] center leads to one electron reduction and formation of $(P)Fe^{II}(NO^+)$, where P denotes a porphyrin,[18] followed by reductive nitrosylation via attack of a nucleophile, viz., a water molecule or hydroxide ion as a general base, on the ferrous nitrosonium complex in aqueous media to produce a ferrous nitrosyl species, viz., $(P)Fe^{II}(NO)$. This process is referred to as reductive nitrosylation and is summarized in reaction 1 and shown in Scheme 1.[9]

$$\begin{array}{l} (P)Fe^{III} + NO \underset{}{\overset{K_{NO}}{\rightleftharpoons}} (P)Fe^{II}(NO^+) \xrightarrow{+ Nu^-} (P)Fe^{II}(NO\text{-}Nu) \\ \qquad\qquad\qquad\qquad\qquad\qquad\qquad\quad \downarrow + NO \\ \qquad\qquad\qquad\qquad\qquad\qquad\qquad\quad (P)Fe^{II}(NO) + NO\text{-}Nu \end{array} \quad (1)$$

Reductive nitrosylation also occurs in nonaqueous solution, in a mixed-solvent system of methanol and water where MeO^- acts as the NO^+ acceptor.[19] The final iron(II) nitrosyl porphyrin products were characterized by various spectroscopic methods, such as UV−vis, EPR, and MCD, and electrochemical methods, such as cyclic voltammetry.[20] Several groups have systematically studied the reductive nitrosylation of water-soluble ferric porphyrins such as TPPS,[7,12] TMPyP,[12−14] and hemoproteins such as ferro- and[21] ferric-cytochrome[22] and met-hemoglobin[23] and met-myoglobin[24] in buffered aqueous solution at various pH conditions; several groups have also investigated the roles of a general base buffer, the hydroxide ion, and nitrite catalysis.[24] A surprising fact is that the reduction of ferric nitrosyl porphyrins, $(P)Fe^{II}(NO^+)$, by NO is catalyzed by nitrite, which is always present as an impurity in deoxygenated aqueous NO solutions. Two plausible mechanisms have been suggested to account for nitrite-catalyzed reductive nitrosylation.[12,13] The observed reaction can proceed via direct nucleophilic attack of nitrite on the electrophilic site of coordinated NO^+ to give $(P)Fe^{II}(N_2O_3)$, which would be a key intermediate species that decomposes to the five-coordinate $(P)Fe^{II}$ complex and N_2O_3. N_2O_3 then rapidly hydrolyzes to nitrite, and the five-coordinate ferrous complex $(P)Fe^{II}$ rapidly binds NO to yield $(P)Fe^{II}(NO)$. The reported rate constant for the binding of NO to ferrous porphyrins and proteins is around 3 orders of magnitude faster than for ferric porphyrins.[25] An alternative pathway involves an outersphere electron-transfer mechanism that occurs between nitrite and coordinated NO^+ on $(P)Fe^{II}(NO^+)$ to form the ferrous nitrosyl compound $(P)Fe^{II}(NO)$ plus a NO_2 radical that rapidly binds NO to produce N_2O_3, followed by hydrolysis to nitrite. Importantly, nitrite is not only present as an impurity in the aqueous NO solution in such a catalytic cycle but is also a reaction product so that the system is in principle autocatalytic. These results led us to further investigate reactions with nitrite and the reaction with NO in the presence of nitrite impurities at various pH for the series of highly water soluble porphyrin complexes studied before.[10,12,13]

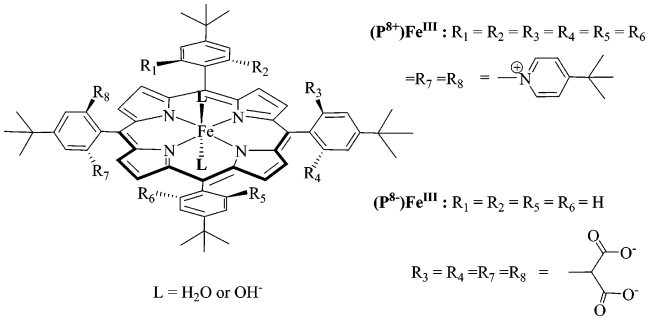

Figure 1. Synthetic Fe^{III} porphyrin complexes $(P^{8+})Fe^{III}(L)_2$ and $(P^{8-})Fe^{III}(L)_2$.

In this context, we studied the reaction of $(P^{8+})Fe^{III}(H_2O)_2$, [5,10,15,20-tetrakis-(4′-*tert*-butyl-2′,6′-bis(4-*tert*-butylpyridine)phenyl)porphinato]iron(III), with NO_2^- at different pH values, temperatures, and pressures. We also studied the reductive nitrosylation reaction following the binding of NO to the highly positively charged ferric porphyrin $(P^{8+})Fe^{III}(H_2O)_2$ and the highly negatively charged ferric porphyrin $(P^{8-})Fe^{III}(H_2O)_2$, [5^4,10^4,15^4,20^4-tetra-*tert*-butyl-5^2,5^6,15^2,15^6-tetrakis-(2,2-biscarboxylato-ethyl)-5,10,15,20-tetraphenylporphyrin]iron(III) (see Figure 1), to produce the ferrous nitrosyl porphyrins $(P^{8-})Fe^{II}(NO)$ and $(P^{8+})Fe^{II}(NO)$, respectively. The reductive nitrosylation reactions were studied at pH 2.0 and 4.0 for $(P^{8+})Fe^{III}(H_2O)_2$, at pH 8.0 for $(P^{8+})Fe^{III}(OH)(H_2O)$, and at pH 7.0 for $(P^{8-})Fe^{III}(H_2O)_2$. The differently charged iron(III) porphyrins were used to compare the reaction properties and reactivity induced by variation of the porphyrin ligand. Variable pH, temperature, and pressure measurements provided detailed kinetic and mechanistic information on the reductive nitrosylation process. The results are compared with kinetic data and mechanistic information

(12) Fernandez, B. O.; Lorkobic, I. M.; Ford, P. C. *Inorg. Chem.* **2004**, *43*, 5393.
(13) Theodoridis, A.; van Eldik, R. *J. Mol. Catal. A: Chem* **2004**, *24*, 197.
(14) Trofimova, N. S.; Safronov, A. Y.; Ikeda, S. *Inorg. Chem.* **2003**, *42*, 1945.
(15) Vilhena, F. S. D. S.; Louro, S. R. W. *J. Inorg. Biochem.* **2004**, *98*, 459.
(16) Bohle, D. S.; Hung, C.-H. *J. Am. Chem. Soc.* **1995**, *117*, 9584.
(17) (a) Han, T. H.; Fukuto, J. M.; Liao, J. C. *Nitric Oxide* **2004**, *10*, 74. (b) Tsuge, K.; DeRosa, F.; Lim, M. D.; Ford, P. C. *J. Am. Chem. Soc.* **2004**, *126*, 6564. (c) Selcuki, C.; van Eldik, R.; Clark, T. *Inorg. Chem.* **2004**, *43*, 2828.
(18) Enemark, J. H.; Feltham, R. D. *Coord. Chem. Rev.* **1974**, *13*, 339.
(19) Wayland, B. B.; Olsen, L. W. *J. Am. Chem. Soc.* **1974**, *96*, 6037.
(20) (a) Barley, M. H.; Takeuchi, K. J.; Meyer, T. J. *J. Am. Chem. Soc.* **1986**, *108*, 5876. (b) Barley, M. H.; Rhodes, M. R.; Meyer, T. J. *Inorg. Chem.* **1987**, *26*, 1746.
(21) Yoshimura, T.; Suzuki, S.; Nakahara, A.; Iwasaki, H.; Masuko, M.; Matsubara, T. *Biochim. Biophys. Acta* **1985**, *831*, 267.
(22) Yoshimura, T.; Suzuki, S. *Inorg. Chim. Acta* **1988**, *152*, 241.
(23) (a) Gow, A. J.; Luchsinger, B. P.; Pawloski, J. R.; Singel, D. J.; Stamler, J. S. *Proc. Natl. Acad. Sci. U.S.A.* **1999**, *96*, 9027. (b) Keilin, D.; Hartree, E. F. *Nature (London)* **1937**, *139*, 548. (c) Chien, J. C. W. *J. Am. Chem. Soc.* **1969**, *91*, 2166.
(24) (a) Hoshino, M.; Maeda, M.; Onischi, R.; Seki, H.; Ford, P. C. *J. Am. Chem. Soc.* **1996**, *118*, 5702. (b) Miranda, K. M.; Nims, R. W.; Thomas, D. D.; Espey, M. G.; Citrin, D.; Bartberger, M. D.; Paolocci, N.; Fukuto, J. M.; Feelisch, M.; Wink, D. A. *J. Inorg. Biochem.* **2003**, *93*, 52.
(25) (a) Laverman, L. E.; Ford, P. C. *J. Am. Chem. Soc.* **2001**, *123*, 11614. (b) Hoshino, M.; Laverman, L.; Ford, P. C. *Coord. Chem. Rev.* **1999**, *187*, 75 and references therein.

reported for other water-soluble iron(III) porphyrins. A feasible mechanism that accounts for the observed reactivity patterns within the series of complexes studied is proposed.

Experimental Section

Materials. The water-soluble porphyrin complexes $Na_7[(P^{8-})Fe^{III}]$[10b] and $[(P^{8+})Fe^{III}]Br_9$[10c] were synthesized and characterized as described in previous papers.[10] Bis-tris, Tris, Hepes,[26] and NaOAc/HOAc were used as buffer solutions and purchased from Sigma-Aldrich. All chemicals used in this study were of analytical grade reagent. The NO gas was purified from impurities of nitrogen oxides such as NO_2 and N_2O_3 by passing through an Ascarite II column (NaOH on silica gel from Sigma-Aldrich) and concentrated NaOH solution and was obtained from Riessner Gase or Linde 93 in a purity of at least 99.5%.

Solution Preparation. All solutions were prepared under strict oxygen-free conditions with Milli-Q water and handled in gastight glassware because of the high oxygen sensitivity of NO and the nitrosyl complexes. Oxygen-free Ar and N_2 were used to prepare deoxygenated solutions. Buffered solutions were prepared with 0.05 M Bis-tris, Tris, Hepes, and NaOAc/HOAc, and solutions at pH 2.0 were prepared with HNO_3. The ionic strength was kept at 0.1 M with $NaClO_4$ and KNO_3.

Measurements. pH measurements were carried out on a Metrohm 623 pH meter equipped with a Sigma glass electrode. UV−vis spectra were recorded on a Shimadzu UV-2100 spectrophotometer equipped with a thermostated cell compartment CDS-260. UV−vis spectra at pressures up to 150 MPa were recorded in a custom-built high-pressure optical cell.[27] Stopped-flow kinetic measurements on the reaction of nitrite and NO with $(P^{8+})Fe^{III}(H_2O)_2$ were carried out using an Applied Photophysics SX-18MV stopped-flow spectrometer. Deoxygenated water solutions of $(P^{8+})Fe^{III}(H_2O)_2$ were rapidly mixed with nitrite and NO solutions containing a certain concentration of nitrite. The observed rate constants and activation parameters for the reactions with nitrite and NO/nitrite were monitored at 435 nm, where the change in absorbance is at a maximum. We measured the rate constants for the conversion $(P^{8+})Fe^{II}(H_2O)(NO^+)$, generated from NO and $(P^{8+})Fe^{III}(H_2O)_2$, to $(P^{8+})Fe^{II}(NO)$. All kinetic experiments were performed under pseudo-first-order conditions, i.e., with at least a 10-fold excess of nitrite and NO. Reported rate constants are mean values of at least five kinetics runs and the uncertainties are quoted on the basis of the standard deviation. High-pressure stopped-flow studies were performed on a custom-built instrument (from 10 to 130 MPa).[28] Kinetic traces were recorded on an IBM-compatible computer and analyzed with the OLIS KINFIT (Bogart, GA) set of programs.

Results and Discussion

Reaction of $(P^{8+})Fe^{III}(H_2O)_2$ with Nitrite. To understand the effect of nitrite on the reactions of the highly charged anionic and cationic Fe^{III} porphyrins with NO, we first studied the reactions of these complexes with nitrite in the absence of NO. Preliminary investigations showed that the cationic complex reacts efficiently with nitrite but that the anionic complex does not bind nitrite at all. For that reason, we focused our studies on the binding of nitrite to the cationic complex. The reaction of different concentrations of HONO/NO_2^- with $(P^{8+})Fe^{III}(H_2O)_2$ led to characteristic spectral changes. The spectrum of $(P^{8+})Fe^{III}(H_2O)_2$ shows absorption maxima at 402 nm ($\epsilon = 8.6 \times 10^4$ M^{-1} cm^{-1}) and 529 nm ($\epsilon = 7.4 \times 10^3$ M^{-1} cm^{-1}) in aqueous solution at pH 2.0 and at 406 nm ($\epsilon = 8.9 \times 10^4$ M^{-1} cm^{-1}) and 529 nm ($\epsilon = 7.4 \times 10^3$ M^{-1} cm^{-1}) at pH 4.0 in a 0.05 M Hepes buffer solution.[10a] Figure 2 shows the reaction of $(P^{8+})Fe^{III}(H_2O)_2$ with various concentrations of HONO/NO_2^-, which leads to a red shift to 424 and 548 nm at pH 2.0 and 4.0, respectively, with several isosbestic points at 416, 480, 535, and 590 nm, indicating that only two complex species exist in equilibrium and that the same product is formed at both pH levels. The spectral changes observed for the formation of the stable nitrite complex $(P^{8+})Fe^{III}(H_2O)(NO_2^-)$ differ from those observed for the formation of $(P^{8+})Fe^{II}(H_2O)(NO^+)$. In the present case, coordinated water is substituted by nitrite with no change in the oxidation state of the metal center, as given in reaction 2.[29,30] For the reaction with NO, FT-IR and Raman data suggest that charge transfer occurs during the binding of NO to form $(P^{8+})Fe^{II}(H_2O)(NO^+)$. The apparent equilibrium constants (K_{HONO} and $K_{NO_2^-}$) for the binding of HONO/NO_2^- to $(P^{8+})Fe^{III}(H_2O)_2$ at pH 2 and 4, respectively, were calculated from the spectral changes (see insets in Figure 2) and found to be $K_{HONO} = (9.9 \pm 0.4) \times 10^3$ M^{-1} at pH 2.0 and $K_{NO_2^-} = (8.8 \pm 0.4) \times 10^4$ M^{-1} at pH 4.0. These values show that NO_2^- is a much stronger nucleophile than HONO, as expected.

$$(P^{8+})Fe^{III}(H_2O) + NO_2^- \underset{k_{-2}}{\overset{k_2}{\rightleftarrows}} (P^{8+})Fe^{III}(H_2O)(NO_2^-) + H_2O \quad (2)$$

The kinetics of the observed reaction was studied under pseudo-first-order conditions, i.e., at least a 10-fold excess of nitrite, as a function of nitrite concentration, pH, temperature, and pressure. As can be seen from Figure 3, plots of k_{obs} vs [total nitrite] are linear, with a slope equal to the rate constant for the formation of $(P^{8+})Fe^{III}(H_2O)(NO_2^-)$ and an intercept close to zero, i.e., $k_{obs} = k_2[NO_2^-] + k_{-2} \approx k_2[NO_2^-]$. The observed second-order rate constant for nitrite binding to $(P^{8+})Fe^{III}(H_2O)_2$, $k_2 = (9.0 \pm 0.2) \times 10^3$ M^{-1} s^{-1} at pH 2.0, is 10-fold lower than the value found at pH 4.0, $k_2 = (85 \pm 4) \times 10^3$ M^{-1} s^{-1}, which accounts for the difference in the overall equilibrium constants reported above. This trend can be accounted for in terms of the lower nucleophilicity of HONO mainly present at pH 2.0, as compared to nitrite mainly present at pH 4.0. A more systematic pH dependence of $k_2 = k_{obs}$/[total NO_2^-] was studied in the range 1.8−4.5, for which the results are

(26) Medzon, E. L.; Gedies, A. *Can. J. Microbiol.* **1971**, *17*, 651.
(27) Spitzer, M.; Gartig, F.; van Eldik, R. *Rev. Sci. Instrum.* **1988**, *59*, 2092.
(28) van Eldik, R.; Gaede, W.; Wieland, S.; Kraft, J.; Spitzer, M.; Palmer, D. A. *Rev. Sci. Instrum.* **1993**, *64*, 1355.
(29) Wanat, A.; Gdula-Argasinska, J.; Rutkowska-Zbik, D.; Witko, M.; Stochel, G.; van Eldik, R. *J. Biol. Inorg. Chem.* **2002**, *7*, 165.
(30) (a) Munro, O. Q.; Scheidt, W. R. *Inorg. Chem.* **1998**, *37*, 2308 (b) Nasri, H.; Goodwin, J. A.; Scheidt, W. R. *Inorg. Chem.* **1990**, *29*, 185.

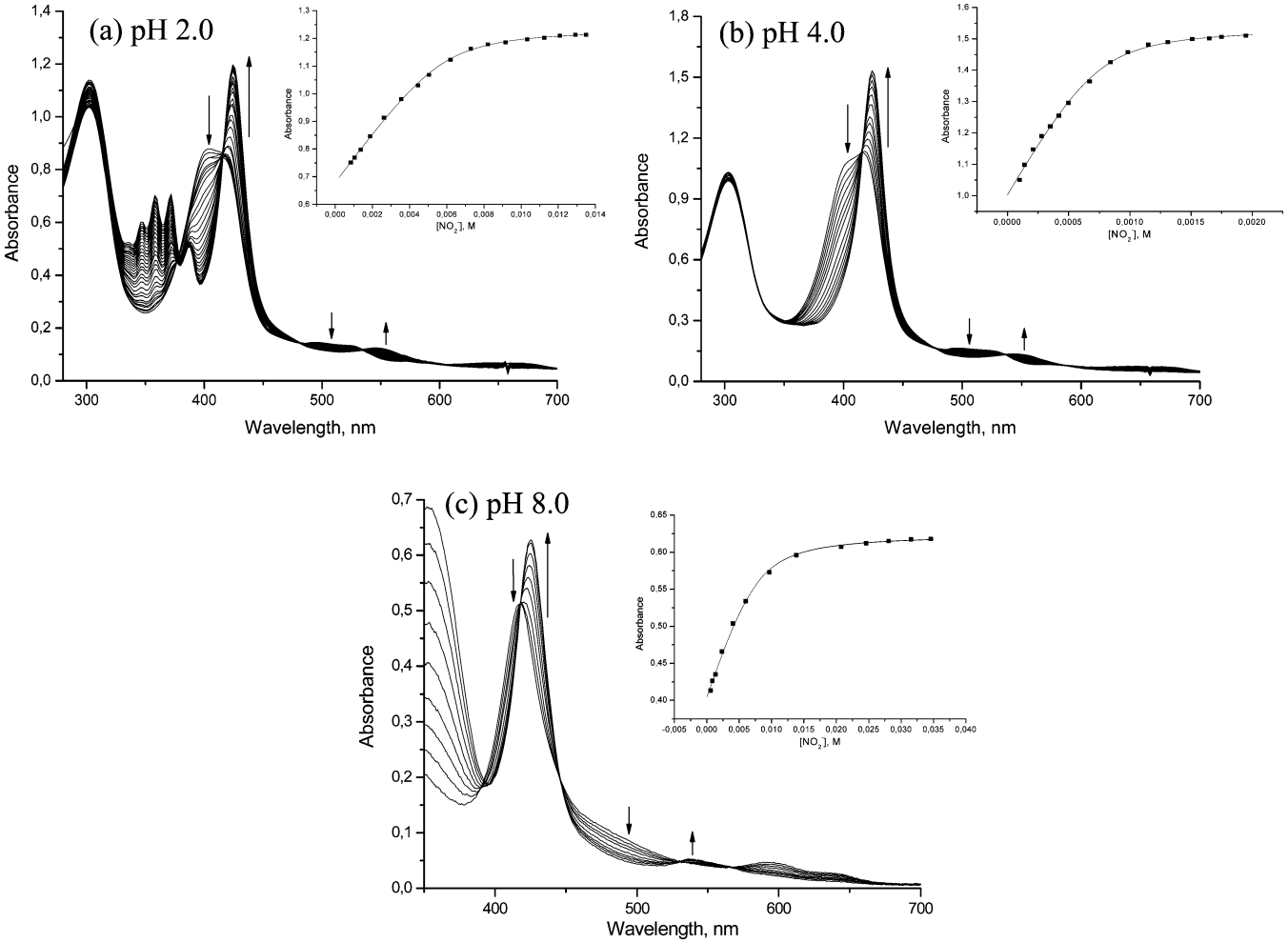

Figure 2. Spectral changes observed during the binding of nitrite at 298 K (a) to $(P^{8+})Fe^{III}(H_2O)_2$, pH 2.0, $[(P^{8+})Fe^{III}]^{9+} = 1.0 \times 10^{-5}$ M, $[NaNO_2] = 1-15$ mM; inset, plot of absorbance vs nitrite concentration from which the equilibrium constant $K_{HONO} = (9.9 \pm 0.4) \times 10^3$ M^{-1} was calculated; (b) to $(P^{8+})Fe^{III}(H_2O)_2$, pH 4.0 (Hepes buffer), $[(P^{8+})Fe^{III}]^{9+} = 1.4 \times 10^{-5}$ M, $[NaNO_2] = 0.5-2$ mM; inset, plot of absorbance vs nitrite concentration from which $K_{NO_2^-} = (8.8 \pm 0.4) \times 10^4$ M^{-1} was calculated; (c) to $(P^{8+})Fe^{III}(OH)(H_2O)$, pH 8.0 (Tris buffer), $[(P^{8+})Fe^{III}]^{9+} = 6.0 \times 10^{-6}$ M, $[NaNO_2] = 0.5-35$ mM; inset, plot of absorbance vs nitrite concentration from which $K_{NO_2^-} = (9.6 \pm 1.5) \times 10^2$ M^{-1} was calculated.

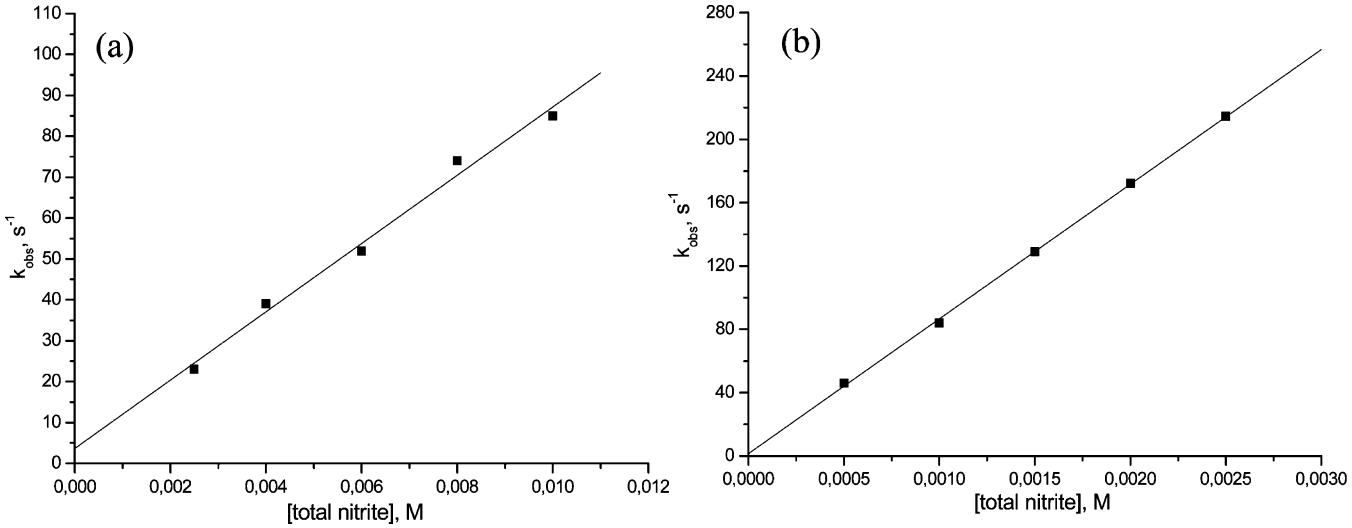

Figure 3. Plot of k_{obs} vs [total nitrite] for nitrite binding to $(P^{8+})Fe^{III}(H_2O)_2$ at (a) pH 2.0 and (b) pH 4.0. Experimental conditions: $[(P^{8+})Fe^{III}]^{9+} = 7.5 \times 10^{-6}$ M, $\lambda_{det} = 430$ nm, $T = 25.0$ °C, $I = 0.1$ M (with KNO_3).

presented in Figure 4. It can be seen from the data that the rate constant for nitrite binding to $(P^{8+})Fe^{III}(H_2O)_2$ decreases and becomes slower on going to lower pH and tends to zero at pH ≤1. On the basis of reactions 3−5, we can express the rate law for the pH dependence of the reaction with nitrite as given in reaction 6.

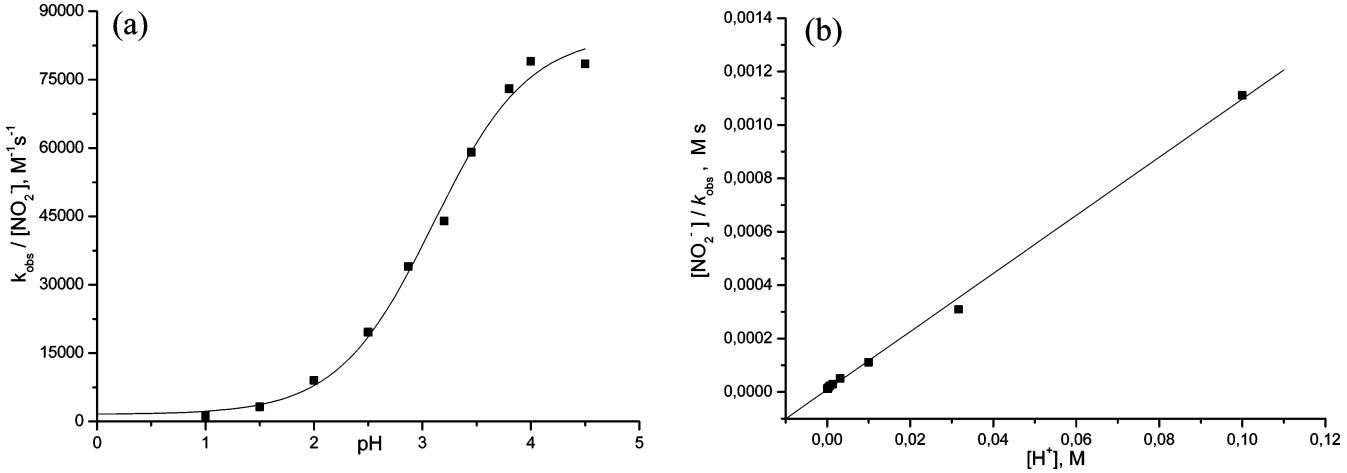

Figure 4. (a) Plot of k_{obs}/[nitrite] vs pH for nitrite binding to $(P^{8+})Fe^{III}(H_2O)_2$ in buffered aqueous solutions in the pH range 1.0−4.5, observed pK_a = 3.10 ± 0.06. (b) Plot of [nitrite]/k_{obs} vs [H^+] to determine K_a and k_2. Experimental conditions: $[(P^{8+})Fe^{III}]^{9+} = 2.0 \times 10^{-5}$ M, λ_{det} = 430 nm, T = 25.0 °C, I = 0.1 M (KNO_3).

$$HONO \overset{K_a}{\rightleftharpoons} NO_2^- + H^+ \quad (3)$$

$$(P^{8+})Fe^{III} + HONO \xrightarrow{k_1} \text{product} \quad (4)$$

$$(P^{8+})Fe^{III} + NO_2^- \xrightarrow{k_2} \text{product} \quad (5)$$

$$k_{obs} = \left\{\frac{k_1[H^+] + k_2K_a}{K_a + [H^+]}\right\}[\text{total } NO_2^-] \quad (6)$$

This rate law can be simplified by using the fact that $k_2 \gg k_1$ (where k_1 has the value of k_2 measured at pH = 2.0), as shown by the data in Figure 4 and rewritten as given in reaction 7. The plot of [total NO_2^-]/k_{obs} vs [H^+] (Figure 4b) is linear with a slope of $1/k_2K_a$ and an intercept of $1/k_2$, from which it follows that $k_2 = 1.14 \times 10^5$ M^{-1} s^{-1} and $K_a = 8.06 \times 10^{-4}$ M, i.e., pK_a = 3.09. The latter value is in close agreement with that determined from a spectrophotometric titration of nitrous acid, viz. pK_a = 3.27 in 0.1 M KNO_3.[31] By combining the values of k_1 and k_2 with the apparent equilibrium constants K_{HONO} and $K_{NO_2^-}$, the rate constants for the dissociation of nitrite (k_{-1} and k_{-2}) were calculated to be 0.83 ± 0.01 and 0.96 ± 0.21 s^{-1} at 25 °C, respectively. Thus the release of nitrite does not significantly depend on pH in the studied range.

$$\frac{[\text{total } NO_2^-]}{k_{obs}} = \frac{1}{k_2} + \frac{[H^+]}{k_2K_a} \quad (7)$$

The temperature dependence of the reaction was studied over the range 5−25 °C at pH 2.0 and 4.0, and the corresponding Eyring plots (Figures S1 and S2, see the Supporting Information) resulted in $\Delta H^{\ddagger}$ and $\Delta S^{\ddagger}$ values of 73 ± 1 kJ mol^{-1} and +75 ± 6 J mol^{-1} K^{-1} at pH 2.0, respectively, and 76 ± 13 kJ mol^{-1} and +103 ± 5 J mol^{-1} K^{-1} at pH 4.0, respectively. The effect of pressure on the reaction of nitrite with $(P^{8+})Fe^{III}(H_2O)_2$ was investigated at pH 2.0 over the pressure range 10−130 MPa, as shown in Figure S1 of the Supporting Information. A summary of all rate and activation parameters is given in Table 1.

Reaction of $(P^{8+})Fe^{III}(OH)(H_2O)$ with Nitrite. $(P^{8+})Fe^{III}(H_2O)_2$ has a pK_a value of 5.0, indicating that the formation of a hydroxo ligated complex with a weakly bound water molecule, $(P^{8+})Fe^{III}(OH)(H_2O)$, occurs at pH >5.0.[10(a)] As can be seen in Figure 2c, the spectra of $(P^{8+})Fe^{III}(OH)(H_2O)$ at 416 nm ($\epsilon = 9.2 \times 10^4$ M^{-1} cm^{-1}) and 595 nm ($\epsilon = 7.2 \times 10^3$ M^{-1} cm^{-1}) on reaction with nitrite at pH 8.0 to yield $(P^{8+})Fe^{III}(OH)(NO_2^-)$ change to 425 nm ($\epsilon = 1.2 \times 10^5$ M^{-1} cm^{-1}) and 537 nm ($\epsilon = 6.4 \times 10^3$ M^{-1} cm^{-1}), respectively. Kinetic data for the reaction with nitrite at pH 8.0 were obtained as for pH 2.0 and 4.0 and are reported in Figure 5. The results for reaction 8 fit the rate law $k_{obs} = k_3[NO_2^-] + k_{-3} \approx k_3[NO_2^-]$ according to the data in Figure 5, from which it follows that $k_3 = (8.5 \pm 0.2) \times 10^2$ M^{-1} s^{-1} at 25 °C. The equilibrium constant $K_{NO_2^-}$ (= k_3/k_{-3}) at pH 8 calculated from the spectral changes observed in Figure 2c has the value (9.6 ± 1.5) × 10^2 M^{-1}, from which it follows that $k_{-3} = 0.89 \pm 0.04$ s^{-1}, which is very close to the dissociation rate constants found at pH 2 and 4.

$$(P^{8+})Fe^{III}(OH)(H_2O) + NO_2^- \underset{k_{-3}}{\overset{k_3}{\rightleftarrows}} (P^{8+})Fe^{III}(OH)(H_2O) + H_2O \quad (8)$$

The temperature and pressure dependence of the reaction were studied at pH 8.0, for which the data are reported in Figure S3 of the Supporting Information, and the activation parameters are summarized in Table 1. The data in Table 1 can be interpreted in a similar way as that reported for the pH dependence of the binding of NO to $(P^{8+})Fe^{III}(H_2O)_2$ in our earlier study.[10a] A comparison of the data is presented in Table 2 for the reactions at pH 2 and 8. At low pH, the reaction with nitrite follows a dissociative interchange (I_d) mechanism as supported by the positive $\Delta V^{\ddagger}$ value, which is in good agreement with that found for the water-exchange reaction and the binding of NO.[10a] The activation volume is larger than that found for the reaction with NO, which can be ascribed to the neutralization of charge (i.e., decrease in

(31) Riordan, E.; Minogue, N.; Healy, D.; O'Driscoll, P.; Sodeau, J. R. *J. Phys. Chem. A* **2005**, *109*, 779 and references therein. An often quoted literature value is pK_a = 3.27.

Table 1. Temperature and Pressure Dependence of the Reaction of Nitrite with $(P^{8+})Fe^{III}(H_2O)_2$ and $(P^{8+})Fe^{III}(H_2O)(OH)$ at 25 °C

		k_{obs} (s^{-1})			
T (°C)	pressure (MPa)	pH 1.0[a]	pH 2.0[b]	pH 4.0[c]	pH 8.0[d]
2.5	0.1	2.8 ± 0.3	4.9 ± 0.4	6.2 ± 0.3	3.9 ± 0.3
5	0.1	4.0 ± 0.4	5.7 ± 0.3	7.8 ± 0.4	5.0 ± 0.5
10	0.1	7 ± 1	10 ± 1	15 ± 2	8 ± 1
15	0.1	13 ± 2	18 ± 1	27 ± 3	12 ± 2
20	0.1	28 ± 2	32 ± 3	46 ± 3	20 ± 2
25	0.1	53 ± 3	54 ± 2	81 ± 1	28 ± 3
2.5	10		4.7 ± 0.2		3.6 ± 0.3
2.5	50		4.1 ± 0.4		3.8 ± 0.1
2.5	90		3.6 ± 0.3		4.0 ± 0.3
2.5	130		3.2 ± 0.3		4.2 ± 0.1
$k_{obs}/[NO_2^-]$ at 25 °C			$(9.0 \pm 0.2) \times 10^3$	$(81 \pm 1) \times 10^3$	$(0.93 \pm 0.04) \times 10^3$
k (M^{-1} s^{-1})[e]			$(8.3 \pm 0.5) \times 10^3$	$(85 \pm 1) \times 10^3$	$(0.85 \pm 0.02) \times 10^3$
$\Delta H^{\ddagger}$ (kJ mol^{-1})		88 ± 3	73 ± 1	76 ± 13	57 ± 1
$\Delta S^{\ddagger}$ (J mol^{-1} K^{-1})		+109 ± 11	+75 ± 6	+103 ± 5	6 ± 5
$\Delta V^{\ddagger}$ (cm^3 mol^{-1})			+7.3 ± 0.4	[f]	−3.0 ± 0.1

[a] $[NO_2^-] = 40$ mM, $\lambda_{det} = 430$ nm. [b] $[NO_2^-] = 6$ mM, $\lambda_{det} = 435$ nm. [c] $[NO_2^-] = 1$ mM, $\lambda_{det} = 435$ nm. [d] $[NO_2^-] = 30$ mM, $\lambda_{det} = 435$ nm was used. [e] Values calculated from the slope of k_{obs} vs $[NO_2^-]$ at 25 °C. [f] It was impossible to measure the activation volume because the reaction was too fast.

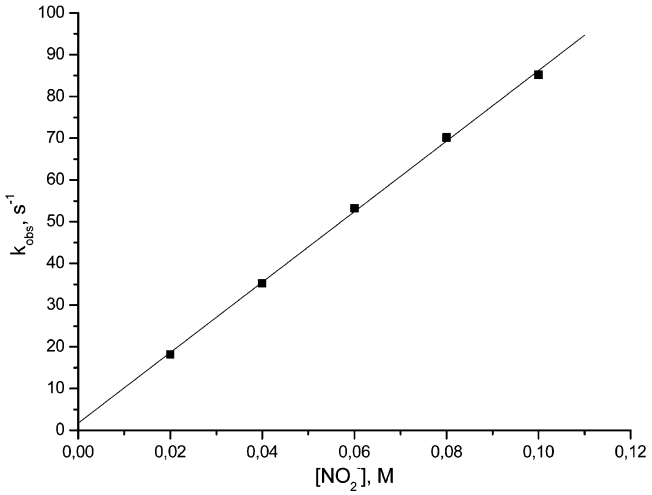

Figure 5. Nitrite concentration dependence of the reaction of $(P^{8+})Fe^{III}(OH)(H_2O)$ with NO_2^-. Experimental conditions: $[(P^{8+})Fe^{III}]^{9+} = 8.5 \times 10^{-6}$ M, $[NO] = 1$ mM, $\lambda_{det} = 435$ nm, $T = 25.0$ °C, $I = 0.1$ M (KNO_3), pH 8.0.

electrostriction) during the formation of $(P^{8+})Fe^{III}(H_2O)(NO_2^-)$. At pH 8.0, the binding of nitrite also follows an associative interchange (I_a) pathway with $(P^{8+})Fe^{III}(OH)(H_2O)$ as judged from the negative activation volume, which is in agreement with that found for the binding of NO.[10a] The more positive (less negative) value can again be ascribed to charge neutralization during the formation of $(P^{8+})Fe^{III}(OH)(NO_2^-)$, which results in a decrease in electrostriction that is accompanied by a volume increase.

Spontaneous Reductive Nitrosylation of $(P^{8-})Fe^{III}$ and $(P^{8+})Fe^{III}$. Exposure of an aqueous solution of $(P^{8-})Fe^{III}(H_2O)_2$ to NO results in rapid characteristic spectral changes and the formation of a Soret band at 427 nm ($\epsilon = 1.5 \times 10^5$ M^{-1} cm^{-1}) and Q-band at 540 nm at pH 7.0 in 0.05 M bis-tris buffer ($I = 0.1$ M),[10a] indicating the formation of $(P^{8-})Fe^{II}(H_2O)(NO^+)$. This species undergoes a subsequent slow reaction with the formation of a Soret band at 414 nm ($\epsilon = 9.6 \times 10^4$ M^{-1} cm^{-1}) and Q-band at 610 nm with clean isosbestic points at 300, 345, 523, and 556 nm, as shown in Figure 6. The final nitrosyl product appeared to be very stable and irreversible on bubbling Ar or N_2 through the solution. This final spectrum is identical to that of the five-coordinate nitrosyl ferrous adduct $(P^{8-})Fe^{II}(NO)$ formed by the addition of NO to the reduced ferrous porphyrin, $(P^{8-})Fe^{II}$, which suggests that $(P^{8-})Fe^{II}(H_2O)(NO^+)$ is converted to $(P^{8-})Fe^{II}(NO)$ via reduction as outlined in reactions 9−11. The concentration of trace impurities of nitrite in aqueous NO solutions is too low to induce the observed reductive nitrosylation reactions (see the following section on nitrite-catalyzed reductive nitrosylation).

$$(P^{8-})Fe^{III}(H_2O)_2 + NO \overset{K_{NO}}{\rightleftharpoons} (P^{8-})Fe^{II}(H_2O)(NO^+) + H_2O \quad (9)$$

$$(P^{8-})Fe^{II}(H_2O)(NO^+) \xrightarrow[+H_2O]{k_{red}} (P^{8-})Fe^{II}(H_2O) + NO_2^- + 2H^+ \quad (10)$$

$$(P^{8-})Fe^{II}(H_2O) + NO \xrightarrow{fast} (P^{8-})Fe^{II}(NO) + H_2O \quad (11)$$

The rapid reaction of $(P^{8-})Fe^{III}(H_2O)_2$ with NO in reaction 9 leads to an equilibrium mixture of $(P^{8-})Fe^{III}(H_2O)_2$ and $(P^{8-})Fe^{II}(H_2O)(NO^+)$; this reaction is followed by the slow nucleophilic attack of water on coordinated NO^+ in reaction 10 to produce nitrite and $(P^{8-})Fe^{II}(H_2O)$, which rapidly binds NO in reaction 11 to yield $(P^{8-})Fe^{II}(NO)$ (the NO binding constant for ferrous porphyrins $\approx 10^9$ M^{-1} s^{-1}).[25] The observed spectral changes are analogous to that reported in the case of $(TPPS)Fe^{III}$ for the formation of the ferrous analogue $(TPPS)Fe^{II}(NO)$ from the ferric nitrosyl porphyrin $(TPPS)Fe^{III}(NO)$.[12] The observed kinetic trace can be fitted with a single-exponential function, as shown in the inset of Figure 6. The [NO] dependence of the observed rate constant for the reductive nitrosylation of $(P^{8-})Fe^{II}(H_2O)(NO^+)$ at pH 7.0 and 25 °C is reported in Figure 7. The observed rate constant increases with increasing [NO] and reaches a limiting value at high [NO]. This is typical for a reaction scheme that consists of a rapid pre-equilibrium followed by a rate-determining step as outlined in reactions 9−11. According to the corresponding rate law in eq 12, a plot of

Table 2. Comparison of the Rate Constants and Activation Parameters for the Binding of NO_2^- and NO to $(P^{8+})Fe^{III}(H_2O)_2$ at pH 2.0 and $(P^{8+})Fe^{III}(OH)(H_2O)$ at pH 8.0 and 25 °C

	$(P^{8+})Fe + NO_2^-$		$(P^{8+})Fe + NO^a$	
	pH 2	pH 8	pH 2	pH 8
$k_{NO_2^-}$ ($M^{-1}\,s^{-1}$)	$(8.3 \pm 0.5) \times 10^3$	$(0.85 \pm 0.02) \times 10^3$		
k_{NO} ($M^{-1}\,s^{-1}$)			$(15.1 \pm 0.9) \times 10^3$	$(1.56 \pm 0.06) \times 10^3$
$\Delta H^{\ddagger}$ (kJ mol^{-1})	73 ± 1	57 ± 1	77 ± 3	41 ± 1
$\Delta S^{\ddagger}$ (J $mol^{-1}\,K^{-1}$)	$+75 \pm 6$	$+6 \pm 5$	$+94 \pm 12$	-45 ± 2
$\Delta V^{\ddagger}$ ($cm^3\,mol^{-1}$)	$+7.3 \pm 0.4$	-3.0 ± 0.1	$+1.5 \pm 0.3$	-13.8 ± 0.4

[a] Data taken from ref 10a.

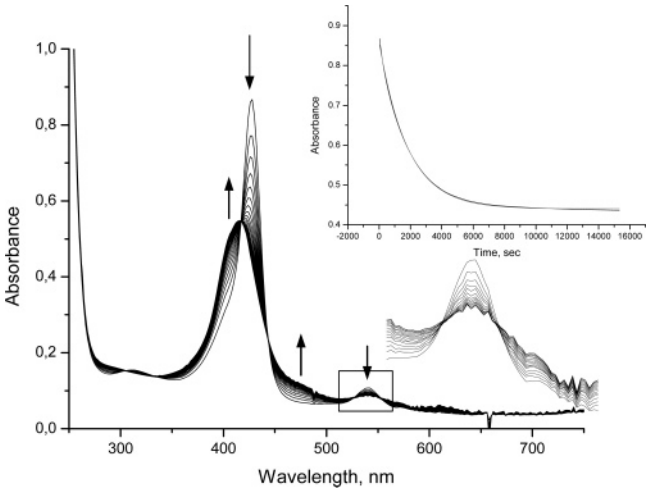

Figure 6. Spectral changes observed following the binding of NO to $(P^{8-})Fe^{III}(H_2O)_2$. Inset: kinetic trace of absorbance at 426 nm vs time fitted to a single-exponential function. Experimental conditions: $[(P^{8-})Fe^{III}]^{7-} = 1 \times 10^{-5}$ M, [NO] = 1 mM, [added NO_2^-] = 0, $T = 25.0$ °C, $I = 0.1$ M with $NaClO_4$, pH = 7.0. The first 10 spectra were taken every 6 min, the next 10 spectra every 9 min, and the rest every 15 min.

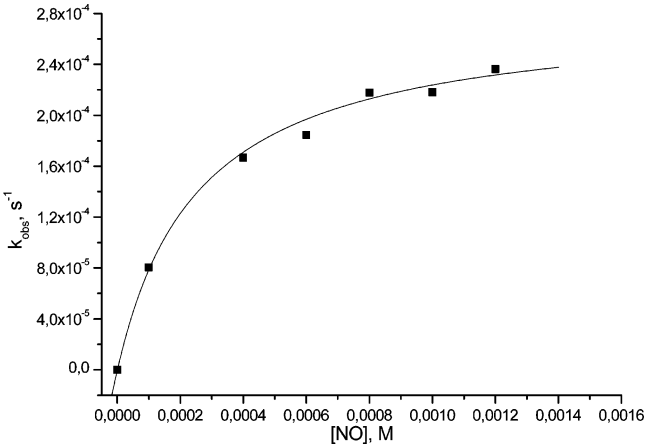

Figure 7. Plot of k_{obs} vs [NO] for the reductive nitrosylation of $(P^{8-})Fe^{II}(H_2O)(NO^+)$. Experimental conditions: $[Fe^{III}(P^{8-})]^{7-} = 2.0 \times 10^{-5}$ M, [NO] in the range 0−1.2 mM, $T = 25.0$ °C, $\lambda_{det} = 430$ nm, $I = 0.1$ M (with $NaClO_4$), pH 7.0.

$(k_{obs})^{-1}$ vs $[NO]^{-1}$ should be linear with a slope $(K_{NO}k_{red})^{-1}$ and an intercept $(k_{red})^{-1}$, from which $K_{NO} = (3.9 \pm 0.3) \times 10^3\ M^{-1}$ and $k_{red} = (2.8 \pm 0.2) \times 10^{-4}\ s^{-1}$ were obtained from Figure S4 of the Supporting Information. The calculated equilibrium constant is in close agreement with the corresponding value $K_{NO} = k_{on}/k_{off} = (3.8 \pm 0.2) \times 10^3\ M^{-1}$ (at 24 °C) determined from laser flash photolysis measurements.[10b] The value of k_{red} is also in a good agreement with that measured directly, viz. $k_{red} = 2.2 \times 10^{-4}\ s^{-1}$, under high [NO] conditions.

$$k_{obs} = \frac{k_{red}K_{NO}[NO]}{1 + K_{NO}[NO]} \qquad (12)$$

The $(P^{8+})Fe^{III}(H_2O)_2$ complex undergoes a similar reaction at pH 2.0 following the binding of NO, but the reduction occurs more rapidly than for $(P^{8-})Fe^{III}(H_2O)_2$, such that the spectral changes for the subsequent reaction were recorded using a rapid-scan technique. After the mixing of $(P^{8+})Fe^{III}(H_2O)_2$ with NO, new bands appear at 422 nm ($\epsilon = 9.5 \times 10^4\ M^{-1}\ cm^{-1}$) and 553 nm at pH 2.0 that indicate the subsequent formation of $(P^{8+})Fe^{II}(NO)$, as shown in Figure 8a. At pH 4.0, the reaction proceeded in the same manner as at pH 2.0 and new bands are formed at 422 nm ($\epsilon = 9.9 \times 10^4\ M^{-1}\ cm^{-1}$) and 553 nm, as shown in Figure 8b. The observed kinetic traces can be fitted with a single-exponential function, as shown in the insets of panels a and b of Figure 8.

Kinetic data for the reductive nitrosylation of $(P^{8+})Fe^{II}(H_2O)(NO^+)$ were measured as a function of [NO] at pH 2.0, for which the results are reported in Figure 9 and Figure S4 of the Supporting Information. The results are very similar to those reported for $(P^{8-})Fe^{III}(H_2O)_2$ in Figure 7 and can be interpreted in the same way in terms of reactions 9−11. A fit of the data according to eq 12 results in $K_{NO} = (5.4 \pm 0.4) \times 10^2\ M^{-1}$ and $k_{red} = (4.0 \pm 0.2) \times 10^{-2}\ s^{-1}$, from which it follows that K_{NO} is in close agreement with the corresponding value $K_{NO} = k_{on}/k_{off} = (5.7 \pm 0.4) \times 10^2\ M^{-1}$ estimated from the kinetic data at 25 °C.[10a] The value of k_{red} is approximately 1×10^2 larger for the reduction of the positively charged ferrous nitrosyl porphyrin than for the negatively charged porphyrin. This is consistent with earlier data reported for the reductive nitrosylation of the corresponding nitrosyl complexes of $(TMPyP^{4+})Fe^{III}$ and $(TPPS^{4-})Fe^{III}$.[12] These differences must be related to the electrophilicity of the Fe(III) center that is affected by the porphyrin environment, which in turn determines the stability of the ferrous nitrosonium intermediate, $(P)Fe^{II}(NO^+)$, and controls the rate of the subsequent reductive nitrosylation reaction. Once $(P)Fe^{II}(NO^+)$ is formed, the subsequent reduction of the nitrosyl ligand can be accelerated by the positively charged electron-withdrawing meso substituents in $(P^{8+})Fe^{II}(NO^+)$ as compared to the electron-donating substituents in $(P^{8-})Fe^{II}(NO^+)$ (see Scheme 2a,b). A similar effect was observed for the cationic complex on going to higher pH where $(P^{8+})Fe^{II}(OH)(NO^+)$ undergoes a subsequent reductive nitrosylation reaction.

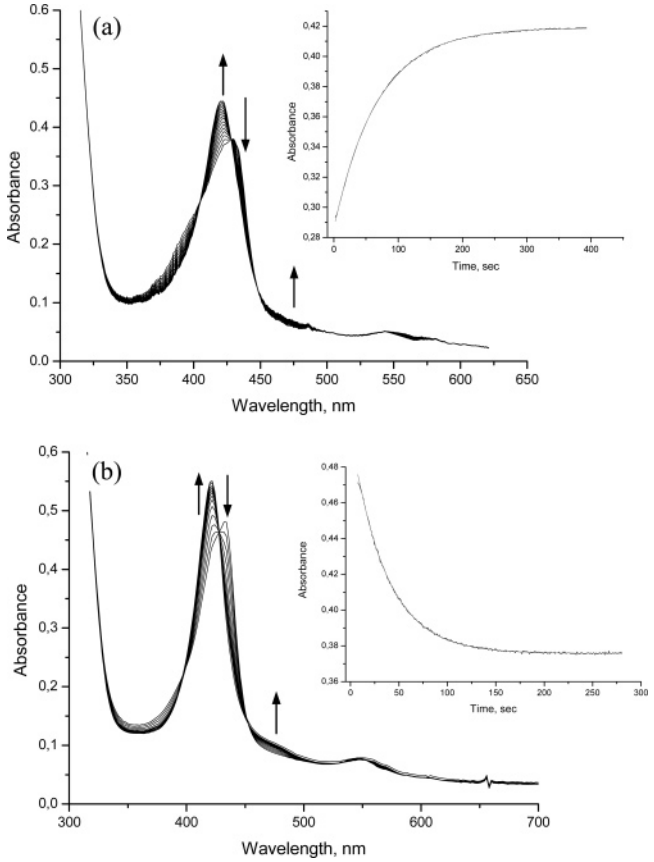

Figure 8. (a) Repetitive scan spectra recorded following the binding of NO to $(P^{8+})Fe^{III}(H_2O)_2$ at pH 2.0. Inset: Kinetic trace at 420 nm fitted with a single-exponential function. Experimental conditions: $[(P^{8+})Fe^{III}]^{9+} = 4.1 \times 10^{-6}$ M, [NO] = 0.6 mM, $\lambda_{det} = 422$ nm, $T = 25.0$ °C, $I = 0.1$ M (with KNO_3). The spectra were recorded every 3 s. (b) Spectral changes recorded following the binding of NO to $(P^{8+})Fe^{III}(H_2O)_2$ at pH 4.0. Conditions: $[(P^{8+})Fe^{III}]^{9+} = 4.8 \times 10^{-6}$ M, [NO] = 1 mM, $T = 25.0$ °C. Spectra were recorded every 5 s. Inset: Observed kinetic trace is observed at 432 nm.

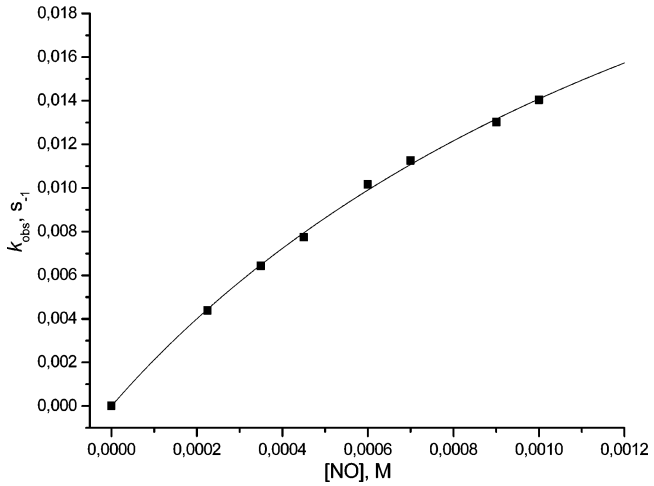

Figure 9. Plot of k_{obs} vs [NO] for the reductive nitrosylation of $(P^{8+})Fe^{II}(H_2O)(NO^+)$. Experimental conditions: $[Fe^{III}(P^{8+})]^{9+} = 3.0 \times 10^{-5}$ M, [NO] in the range 0−1.0 mM, $T = 25.0$ °C, $\lambda_{det} = 431$ nm, $I = 0.1$ M (with KNO_3), pH 2.0.

Figure 10 shows the spectral changes that result from mixing $(P^{8+})Fe^{III}(OH)(H_2O)$ with an aqueous NO solution at pH 8. The decrease in absorbance at 416 and 598 nm is accompanied by an increase in absorbance at 422 nm ($\epsilon =$

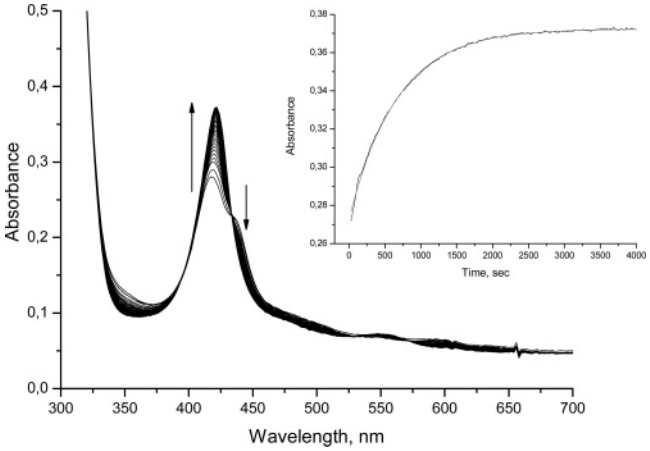

Figure 10. Repetitive scan spectra recorded following the binding of NO to $(P^{8+})Fe^{III}(H_2O)(OH)$ at pH 8.0. Inset: Kinetic trace of absorbance vs time at 422 nm fitted with a single-exponential function. Experimental conditions: $[(P^{8+})Fe^{III}]^{9+} = 7.5 \times 10^{-6}$ M, [NO] = 1 mM, $T = 25.0$ °C, pH 8.0, $I = 0.1$ M (KNO_3). The spectra were recorded every 25 s.

Scheme 2

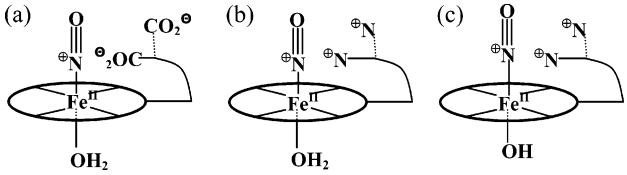

1.1×10^5 M^{-1} cm^{-1}) and 553 nm and features the formation of $(P^{8+})Fe^{II}(NO)$. Hence, the coordination of NO and the subsequent reductive nitrosylation of $(P^{8+})Fe^{II}(OH)(NO^+)$ are suggested to occur according to reactions 13−15 in a manner similar to that outlined in reactions 9−11.

$$(P^{8+})Fe^{III}(OH)(H_2O) + NO \overset{K_{NO}}{\rightleftharpoons} (P^{8+})Fe^{II}(OH)(NO^+) + H_2O \quad (13)$$

$$(P^{8+})Fe^{II}(OH)(NO^+) \xrightarrow[OH^-]{k_{red}} (P^{8+})Fe^{II}(OH) + NO_2^- + H^+ \quad (14)$$

$$(P^{8+})Fe^{II}(OH) + NO \xrightarrow{fast} (P^{8+})Fe^{II}(NO) + OH^- \quad (15)$$

The [NO] dependence of the reductive nitrosylation of $(P^{8+})Fe^{II}(OH)(NO^+)$ was studied, and the results are displayed in Figure 11 and Figure S4 of the Supporting Information. A fit of the data to eq 12 resulted in $K_{NO} = (2.8 \pm 0.3) \times 10^2$ M^{-1} and $k_{red} = (4.4 \pm 0.7) \times 10^{-3}$ s^{-1}. The obtained value for K_{NO} is in a good agreement with the corresponding value $K_{NO} = k_{on}/k_{off} = (2.5 \pm 0.3) \times 10^2$ M^{-1} obtained from stopped-flow measurements at 25 °C.[10a]

The measured k_{red} value for $(P^{8+})Fe^{II}(OH)(NO^+)$ at pH 8.0 indicates that the reaction is 10 times slower than for $(P^{8+})Fe^{II}(H_2O)(NO^+)$ under similar experimental conditions, which can be accounted for in terms of the effect of the OH^- group in the position trans to NO^+ that will induce electron density onto the nitrosyl ligand and reduce its electrophilic character. A pictorial presentation of the suggested electronic effects is presented in Scheme 2, in which (a) shows the stabilization of the nitrosyl complex by the increased electron

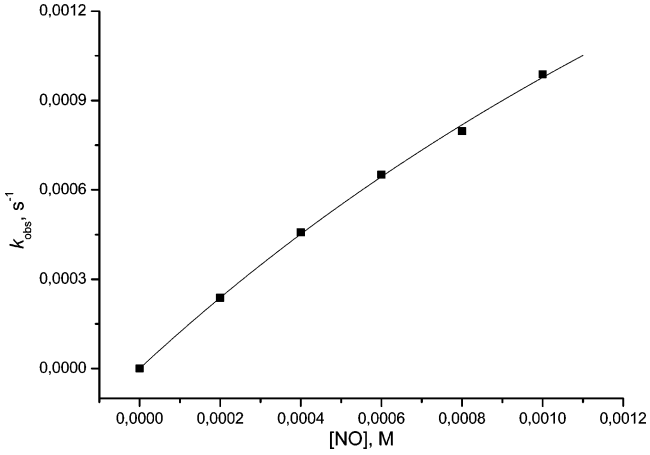

Figure 11. Plot of k_{obs} vs [NO] for the reductive nitrosylation of $(P^{8+})Fe^{II}(OH)(NO^+)$. Experimental conditions: $[Fe^{III}(P^{8+})]^{9+} = 7.0 \times 10^{-6}$ M, [NO] in the range 0−1.0 mM, $T = 25.0$ °C, $\lambda_{det} = 422$ nm, $I = 0.1$ M (KNO_3), pH 8.0.

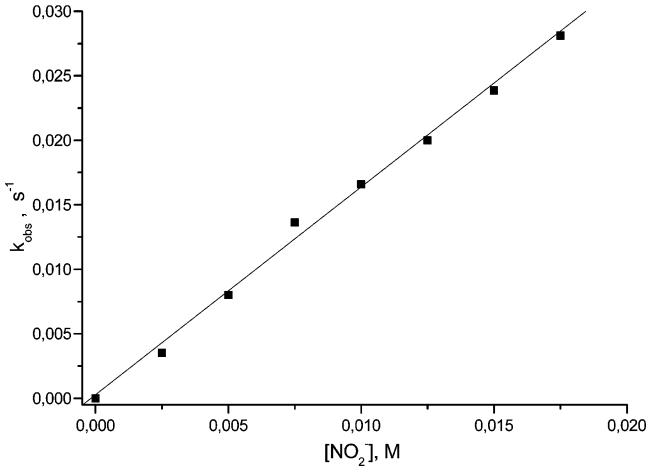

Figure 12. Nitrite concentration dependence of the reductive nitrosylation of $(P^{8-})Fe^{II}(H_2O)(NO^+)$. Experimental conditions: $[Fe^{III}(P^{8-})]^{7-} = 2.0 \times 10^{-5}$ M, [NO] = 1 mM, $T = 25.0$ °C, $\lambda_{det} = 426$ nm, $I = 0.1$ M (with $NaClO_4$), pH 7.0.

density at the Fe(II) center of $(P^{8-})Fe^{II}(H_2O)(NO^+)$ and the influence of the negatively charged porphyrin substituents; (b) indicates the opposite effect caused by the influence of positively charged substituents in $(P^{8+})Fe^{II}(H_2O)(NO^+)$; and (c) shows the trans-labilizing effect caused by the OH^- ligand in $(P^{8+})Fe^{II}(OH)(NO^+)$.

Nitrite-Catalyzed Reductive Nitrosylation of $(P^{8-})Fe^{III}$ and $(P^{8+})Fe^{III}$. The spontaneous reductive nitrosylation reactions outlined in reaction schemes 9−11 and 13−15 suggest that the produced nitrite could subsequently catalyze the reductive nitrosylation reactions. To investigate this further, we performed a detailed study of the nitrite-catalyzed reductive nitrosylation process by introducing larger concentrations of nitrite into the solutions. Reductive nitrosylation of $(P^{8-})Fe^{II}(H_2O)(NO^+)$ and $(P^{8+})Fe^{II}(H_2O)(NO^+)$ is accelerated significantly on addition of nitrite and depends on the selected pH, as illustrated by the kinetic data reported in Figures 12 and 13, respectively (the observed spectral changes are shown in Figures S9 and S10 of the Supporting Information). It should be noted that trace impurities of nitrite in aqueous solutions of NO are too low to induce reductive

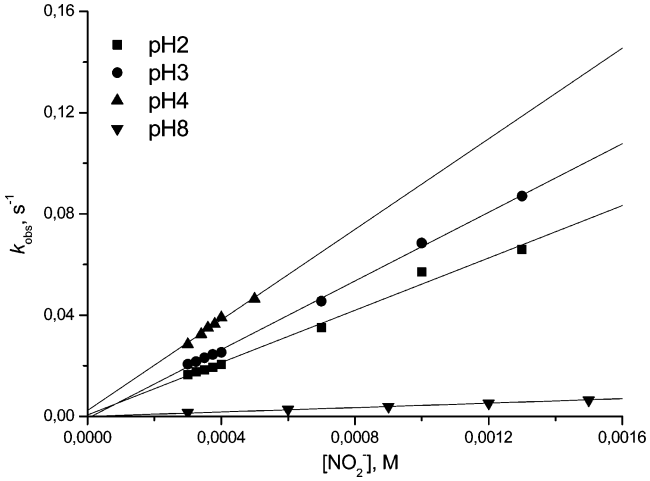

Figure 13. Nitrite concentration dependence of the reductive nitrosylation of $(P^{8+})Fe^{II}(H_2O)(NO^+)$ and $(P^{8+})Fe^{II}(OH)(NO^+)$ at pH 2.0, 3.0, 4.0, and 8.0. Experimental conditions: Nitric acid used for pH 2.0, 0.05 M Hepes buffer for pH 3.0 and 4.0, and Tris buffer for pH 8.0; $[(P^{8+})Fe^{III}]^{9+} = 7.5 \times 10^{-6}$ M, [NO] = 1 mM, $T = 25.0$ °C, $\lambda_{det} = 431$ nm, $I = 0.1$ M (with KNO_3). In these experiments, the indicated nitrite concentration includes the concentration of nitrite impurities present in aqueous NO solutions.

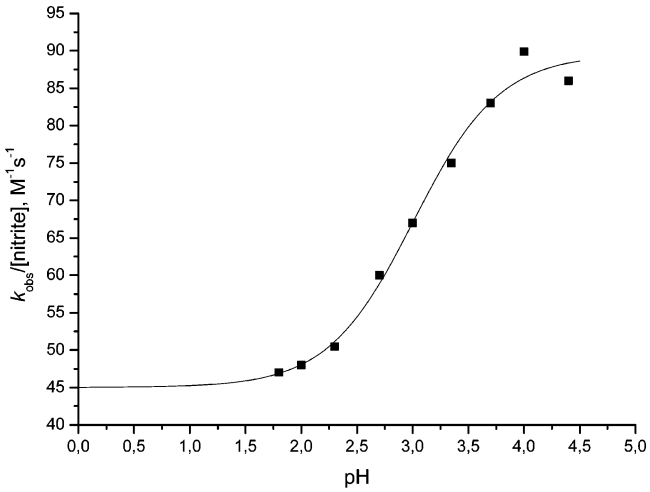

Figure 14. Plot of k_{obs}/[nitrite] vs pH for the reductive nitrosylation of $(P^{8+})Fe^{II}(H_2O)(NO^+)$ in buffered aqueous solutions in the pH range 1.8−4.5. Experimental conditions: $[(P^{8+})Fe^{III}]^{9+} = 2.0 \times 10^{-5}$ M, [NO] = 1 mM, $T = 25.0$ °C, $\lambda_{det} = 431$ nm, $I = 0.1$ M (with KNO_3). Determined $pK_a = 3.00 \pm 0.07$.

nitrosylation of $(P^{8-})Fe^{II}(H_2O)(NO^+)$ under these conditions. The observed rate constant for nitrite-induced reductive nitrosylation of $(P^{8-})Fe^{II}(H_2O)(NO^+)$ at pH 7.0 depends linearly on the nitrite concentration with an observed second-order rate constant of 1.6 ± 0.1 M^{-1} s^{-1} (Figure 12). Similar dependencies were found for the reaction with $(P^{8+})Fe^{II}(H_2O)(NO^+)$ in the pH range 2−8 (Figure 13). The observed second-order rate constant has values of 55 ± 3 and 85 ± 1 M^{-1} s^{-1} at pH 2 and 4, respectively, whereas the value at pH 8 is much smaller. The increase in rate constant with increasing pH was studied in more detail in the range 1.8−4.5. The plot of k_{obs}/[nitrite] vs pH presented in Figure 14 clearly fits a sigmoidal function corresponding to a pK_a value of 3.00 ± 0.07, which is very close to the pK_a value of HONO in 0.1 M KNO_3.[31] From a fit of the data, it follows that nitrite has approximately two times the catalytic activity

of HONO and that both contribute in the studied pH range. The decrease in the catalytic effect observed at pH 8 must be related to the influence of the hydroxy ligand that reduces the electrophilic character of the trans coordinated NO^+.

According to the reaction sequence proposed for the reductive nitrosylation process in Scheme 1, the observed rate constant can be expressed as shown in eq 16. Because K_{NO} and [NO] are known under the selected experimental conditions, the experimental k_{obs} values could be converted to the corresponding k_{nit} values, summarized in Table 3 as a function of temperature and pressure for the studied complexes at different pH values. The activation parameters were estimated in the usual way, for which the corresponding straight line plots are reported in Figures S5−S8 of the Supporting Information.

$$k_{obs} = \frac{k_{nit}K_{NO}[NO_2^-][NO]}{1 + K_{NO}[NO]} \qquad (16)$$

Suggested Mechanism and Comparison of Iron(III) Porphyrins. The results of this study clearly demonstrate the important role of the overall charge on the porphyrin ligand and the metal center in controlling the rate of the reductive nitrosylation reaction. In the case of the $(P^{8-})Fe^{II}(H_2O)(NO^+)$ complex, the overall negative charge on the porphyrin strongly reduces the positive charge on the nitrosyl ligand, which also shows up in the relatively high pK_a value of the $(P^{8-})Fe^{III}(H_2O)_2$ complex. In contrast, reductive nitrosylation of $(P^{8+})Fe^{II}(H_2O)(NO^+)$ is 1×10^2 faster and is ascribed to the higher electrophilicity of the coordinated NO^+. This also shows up in the much lower pK_a value of $(P^{8+})Fe^{III}(H_2O)_2$. In the case of $(P^{8+})Fe^{II}(H_2O)(NO^+)$, the reaction is sensitive to the nature of the reactant, viz. HONO or NO_2^-, and deprotonation of the coordinated water molecule results in a lowering of the electrophilicity of the coordinated NO^+ and a slower reaction. These effects suggest that HONO and NO_2^- catalyze the reductive nitrosylation reaction through direct nucleophilic attack on coordinated NO^+ in a rate-determining step to form an intermediate $Fe^{II}-N_2O_3$ complex, which subsequently dissociates N_2O_3 and binds NO in a ligand exchange process to form the final $(P^n)Fe^{II}(NO)$ complex. The released N_2O_3 undergoes rapid hydrolysis to form HONO or NO_2^-, depending on the pH of the solution. The mechanistic details are shown in Scheme 3. The suggested mechanism is in agreement with the rate law in eq 16, and the reported activation parameters for k_{nit} (summarized in Table 4) can now be used to reveal further mechanistic details of the catalytic process.

Thermal and pressure activation parameters for the reductive nitrosylation process were determined at pH 7 for $(P^{8-})Fe^{II}(H_2O)(NO^+)$ and at pH 2, 4, and 8 for $(P^{8+})Fe^{II}(H_2O)(NO^+)$ and $(P^{8-})Fe^{II}(OH)(NO^+)$. The activation entropy and volume data for the reductive nitrosylation of $(P^{8-})Fe^{II}(H_2O)(NO^+)$ are significantly negative and in line with rate-determining bond formation between coordinated NO^+ and NO_2^-. The bond-formation process is expected to be accompanied by some charge neutralization, which will cause a decrease in electrostriction and partially offset the negative

Table 3. Temperature and Pressure Dependence of the Nitrite-Catalyzed Reductive Nitrosylation Reactions of $(P^{8-})Fe^{II}(H_2O)(NO^+)$, $(P^{8+})Fe^{II}(H_2O)(NO^+)$, and $(P^{8+})Fe^{II}(OH)(NO^+)$ at 25 °C[a]

T (°C)	pressure (MPa)	$(P^{8-})Fe^{II}(H_2O)(NO^+)$, pH 7.0		$(P^{8+})Fe^{II}(H_2O)(NO^+)$, pH 2.0		$(P^{8+})Fe^{II}(H_2O)(NO^+)$, pH 4.0[b]		$(P^{8+})Fe^{II}(OH)(NO^+)$, pH 8.0	
		$k_{obs} \times 10^3$ (s^{-1})	k_{nit} ($M^{-1}s^{-1}$)	$k_{obs} \times 10^3$ (s^{-1})	k_{nit} ($M^{-1}s^{-1}$)	$k_{obs} \times 10^3$ (s^{-1})	k_{nit} ($M^{-1}s^{-1}$)	$k_{obs} \times 10^3$ (s^{-1})	k_{nit} ($M^{-1}s^{-1}$)
5	0.1			5 ± 1	12 ± 2	6 ± 1	31 ± 4		
10	0.1			9 ± 1	23 ± 2	11 ± 1	52 ± 5		
15	0.1	1.2 ± 0.2	0.9 ± 0.1	17 ± 1	46 ± 2	18 ± 1	92 ± 5		
20	0.1	1.8 ± 0.3	1.4 ± 0.2	38 ± 2	99 ± 5	31 ± 2	163 ± 9		
25	0.1	2.4 ± 0.2	2.1 ± 0.2	58 ± 2	161 ± 6	45 ± 2	251 ± 10	4.3 ± 0.6	26 ± 3
30	0.1	3.4 ± 0.4	3.2 ± 0.3					7.6 ± 0.3	39 ± 2
35	0.1	4.6 ± 0.4	5.1 ± 0.5					11.5 ± 0.9	59 ± 4
40	0.1							15.6 ± 0.8	81 ± 5
25	10	0.6 ± 0.1[c]	0.9 ± 0.1	59 ± 2	165 ± 6	47 ± 3	263 ± 11	2.5 ± 0.2[d]	44 ± 3
	50	0.7 ± 0.1[c]	1.0 ± 0.1	52 ± 3	146 ± 9	40 ± 2	223 ± 9	2.4 ± 0.1[d]	43 ± 2
	90	1.0 ± 0.1[c]	1.2 ± 0.1	48 ± 3	134 ± 8	32 ± 2	177 ± 10	2.3 ± 0.2[d]	41 ± 3
	130	1.5 ± 0.2[c]	1.5 ± 0.2	42 ± 2	116 ± 6	26 ± 2	147 ± 10	2.2 ± 0.2[d]	40 ± 3
		$(P^{8-})Fe^{II}(H_2O)(NO^+)$, pH 7.0		$(P^{8+})Fe^{II}(H_2O)(NO^+)$, pH 2.0		$(P^{8+})Fe^{II}(H_2O)(NO^+)$, pH 4.0[a]		$(P^{8+})Fe^{II}(OH)(NO^+)$, pH 8.0	
$\Delta H^{\ddagger}$ (kJ mol^{-1})		60 ± 2		90 ± 3		73 ± 2		68 ± 1	
$\Delta S^{\ddagger}$ (J $mol^{-1}K^{-1}$)		−36 ± 7		+99 ± 10		+92 ± 7		+5 ± 2	
$\Delta V^{\ddagger}$ (cm^3 mol)		−8.6 ± 0.4		+7.2 ± 0.5		+12.3 ± 0.7		+2.2 ± 0.2	

[a] For $(P^{8-})Fe^{II}(H_2O)(NO^+)$ and $(P^{8+})Fe^{II}(H_2O)(NO^+)$, [NO] = 1 mM and $[NO_2^-]$ = 1 mM for both temperature- and pressure-dependent experiments. [b] [NO] = 1 mM, $[NO_2^-]$ = 0.5 mM. [c] Measured at 15 °C. [d] [NO] = 0.5 mM, $[NO_2^-]$ = 0.5 mM. All kinetic traces were recorded at 431 nm.

Table 4. Comparison of Rate and Activation Parameters for the Nitrite-Catalyzed Reductive Nitrosylation Reaction of a Series of $(P)Fe^{II}(H_2O)(NO^+)$ Complexes

porphyrin type	porphyrin charge	pK_a[a]	pH	slope[b] ($M^{-1}s^{-1}$)	$k_{nit,25°C}$ ($M^{-1}s^{-1}$)	$\Delta H^{\ddagger}$ (kJ mol^{-1})	$\Delta S^{\ddagger}$ (J $mol^{-1}K^{-1}$)	$\Delta V^{\ddagger}$ ($cm^3 mol^{-1}$)
$(P^{8+})Fe$	+8	5.0	2	55 ± 3	155 ± 8	90 ± 3	+99 ± 10	+7.2 ± 0.5
$(P^{8+})Fe$	+8	5.0	4	89 ± 1	242 ± 3	73 ± 2	+92 ± 7	+12.3 ± 0.7
$(P^{8+})Fe$	+8	5.0	8	4.3 ± 0.1	22 ± 1	68 ± 1	+5 ± 2	+2.2 ± 0.2
$(TMPyP^{4+})Fe$[c]	+4	5.5	4	15.0 ± 0.1	42 ± 1	88 ± 2	+92 ± 6	+8.8 ± 0.1
$(TMPyP^{4+})Fe$[d]	+4	5.5	5	25 ± 1	83 ± 3			
$(TPPS^{4-})Fe$[d]	−4	7.0	5	2.2 ± 0.1	3.1			
$(P^{8-})Fe$	−8	9.2	7	1.6 ± 0.1	2.1 ± 0.2	60 ± 2	−36 ± 7	−8.6 ± 0.4

[a] pK_a value of the corresponding di-aqua complex. [b] Value calculated from k_{obs} vs $[NO_2^-]$ at constant [NO]. [c] Measured at 15 °C, taken from ref 13. [d] Taken from ref 12.

Scheme 3. Suggested Mechanism for the Nitrite-Catalyzed Reductive Nitrosylation of Nitrosyl Complex $[(P)Fe^{II}(NO^+)]$ According to an Innersphere Mechanism

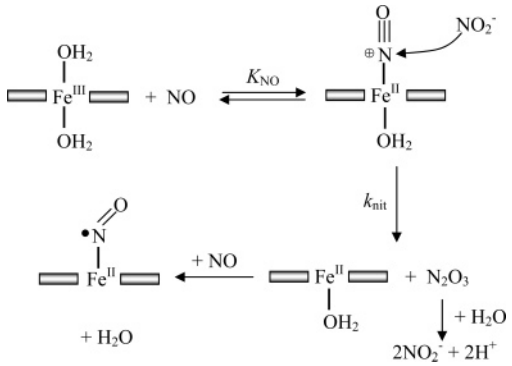

intrinsic entropy and volume contributions. As argued above, the electrophilicity of coordinated NO^+ in this complex is not expected to be that high because of the overall negative charge on the porphyrin, such that the decrease in electrostriction that accompanies bond formation can only partially compensate for the intrinsic contributions arising from bond formation. In the case of the $(P^{8+})Fe^{II}(H_2O)(NO^+)$ complex, however, these activation parameters show large positive values at both pH 2 and 4, indicating that a major decrease in electrostriction during bond formation between coordinated NO^+ and $HONO/NO_2^-$ must be responsible for these values. The electrophilic character of coordinated NO^+ in this complex is expected to be much higher than in the case of the anionic complex, with the result that charge neutralization during the interaction with HONO and NO_2^- is expected to play a major role. This trend is also seen clearly when comparing the activation entropy and volume values found at pH 2 and 4 for the reductive nitrosylation by HONO and NO_2^-, respectively. The more positive values at pH 4 can be ascribed to a larger contribution coming from a decrease in electrostriction that will be accompanied by the release of more solvent molecules, i.e., an increase in entropy and volume, attributable to a more-effective charge-neutralization process. On going to the data for the same reaction at pH 8, both the activation entropy and volume are much smaller (both close to zero) and demonstrate that the decrease in electrostriction almost fully compensates the intrinsic entropy and volume contributions expected for the bond-formation process. This is fully in line with arguments presented above in that the presence of the hydroxo ligand clearly decreases the electrophilicity of coordinated NO^+. Thus the reported activation parameters are fully in line with the mechanistic interpretation offered on the basis of the trends in the observed rate constants for the reductive nitrosylation process as a function of overall charge on the porphyrin and the pH of the solution by which coordinated water is deprotonated in the case of the cationic complex. The subsequent reactions in Scheme 3 are all proposed to be non-rate-determining steps and as such do not affect the reported rate and activation parameters.

The results of the present study are compared to those reported for related systems in Table 4. The values of k_{nit} decrease steadily along the series of complexes $(P^{8+})Fe^{III} > (TMPyP^{4+})Fe^{III} > (TPPS^{4-})Fe^{III} > (P^{8-})Fe^{III}$, i.e., with decreasing overall charge on the porphyrin. Electron-donating substituents on the porphyrin slow the reductive nitrosylation process, whereas electron-withdrawing substituents accelerate the reaction, suggesting that they induce the formation of $(P)Fe^{II}(H_2O)(NO^+)$ and increase the electrophilicity of coordinated NO^+. Activation entropies and activation volumes for reductive nitrosylation of cationic complexes of the type $(P^{n+})Fe^{II}(H_2O)(NO^+)$ are all significantly positive, whereas those for the anionic complex $(P^{8-})Fe^{II}(H_2O)(NO^+)$ are significantly negative. This supports the trends discussed above and can be correlated with the electrophilicity of coordinated NO^+, which in turn controls the contribution of changes in electrostriction that accompanies bond formation between coordinated NO^+ and $HONO/NO_2^-$. The consistency within the series of available data further supports the validity of the suggested mechanism, as outlined in Scheme 3. The results of the present study clearly support the operation of an innersphere electron-transfer mechanism, which is favored over the alternative outersphere electron-transfer mechanism discussed for a number of systems as recently reviewed by Ford and co-workers.[9,12]

Acknowledgment. The authors gratefully acknowledge financial support from the Deutsche Forschungsgemeinschaft within SFB 583 "Redox-Active Metal Complexes" and the European Commission within RTN Contract MRTN-CT-2003-503864. We thank Dr. Norbert Jux and his group (Institute for Organic Chemistry, University of Erlangen-Nürnberg) for providing samples of the porphyrin complexes investigated in this study.

Note Added after ASAP Publication. This article was released ASAP on July 4, 2006, with an error in Figure 4b and incorrect units in line 7 of the paragraph below eq 6. The correct version was posted on July 7, 2006.

Supporting Information Available: Figures S1−S8 present the temperature and pressure dependencies of the individual reactions studied, as well as plots of $(k_{obs})^{-1}$ vs $[NO]^{-1}$ for the reductive nitrosylation reactions reported in Figures 7, 9, and 11. The spectral changes observed for the reductive nitrosylation of $(P^{8-})Fe^{II}(H_2O)(NO^+)$ and $(P^{8+})Fe^{II}(H_2O)(NO^+)$ in the presence of nitrite are shown in Figures S9 and S10. This information is available free of charge via the Internet at http://pubs.acs.org.

IC0603104